How spectral fittings of stellar clusters are affected by the wavelength range used

L.R. Vega-Neme[1,2] & A.V. Ahumada[1,3]

[1] *Observatorio Astronómico de Córdoba, UNC, Argentina*
[2] *Instituto de Astronomía Teórica y Experimental, CONICET–UNC, Argentina*
[3] *Consejo Nacional de Investigaciones Científicas y Técnicas, Argentina*

Received: 09 February 2024 / Accepted: 05 June 2024

Resumen / Star clusters (SCs) are excellent laboratories to test stellar populations, as well as to determine their key properties such as age (t) and metallicity ([Fe/H]). For distant (extragalactic) SCs only integrated spectra are available, and one of the most powerful methods to study these properties is through synthesis modeling. Although this method is very useful, there are several limitations in the results of the models based on spectral synthesis. Here we apply this technique to spectra of Large Magellanic Cloud Star Clusters for different spectral coverage using the synthesis code `Starlight`, in order to explore the dependence of the stellar population parameters with the wavelength ranges used.

Abstract / Los cúmulos estelares (CE) son excelentes laboratorios para estudiar las poblaciones estelares, y para determinar sus propiedades principales como edad (t) y metalicidad ([Fe/H]). Para CE distantes (extragalácticos) se dispone sólo de espectros integrados, y uno de los métodos más poderosos para estudiar estas propiedades es a través de la síntesis espectral. Aunque este método es de gran utilidad, existen varias limitaciones de los resultados basados en la síntesis espectral. Aplicamos esta técnica a espectros de cúmulos estelares de la Nube Mayor de Magallanes para diferentes regiones espectrales usando el código `Starlight`, a fin de explorar la dependencia de los parámetros de las poblaciones estelares con el rango espectral adoptado.

Keywords / Magellanic Clouds — galaxies: star clusters: general — techniques: spectroscopic — methods: data analysis

1. Background and Goals

Stellar clusters (SC) are among the most natural laboratories to study the evolution of stars and stellar populations. To infer their main properties such as age and metallicity, color-magnitude diagrams are very useful when individual stars are identified. On the other hand, integrated light could offer the opportunity of measure spectral indices and colors. The advent of evolutionary synthesis models allowed to fit the observed integrated spectra in all the spectral range available, thus differentiating from the methods which involved only certain wavelength or indices. This is a powerful technique since it is possible to infer the stellar populations involved as well as their global properties (Cid Fernandes et al., 2005). Although the spectral synthesis was widely used to study the stellar populations of normal and active galaxies (Vega Neme, 2009), it was little used in SC spectra (Ahumada et al., 2019).

Although its availability to study stellar populations, the spectral synthesis has a not-so-obvious limitation, related to the spectral range used, which could give false determinations of age, metallicity and/or extinction. The motivation for this behaviour is that for limited wavelength coverage the models with different metallicity could provide statistically indistinguishable fits (Cid Fernandes & González Delgado, 2010). This situation is particularly critical when using only the blue spectral range, and becomes more important for older stellar populations.

To analyse this behaviour in detail, we apply spectral synthesis to a sample of SC spectra by varying the spectral coverage in the fittings. This way, we explore the dependence of the stellar population parameters with the wavelength ranges used. Here, we present our results of this methodology for the SC NGC 2136 located in the Large Magellanic Cloud (LMC).

2. Spectral Synthesis

We took spectra from the WiFeS Atlas of Galactic Globular cluster Spectra (WAGGS; Usher et al., 2017), which contains spectra of 64 Milky Way and 3 Fornax globular clusters, plus 14 LMC and 5 Small Magellanic Cloud (SMC) SC. WAGGS observations correspond to integrated spectra of the central 25x38 arcsec region of the clusters in 5 gratings at R=6800. We gathered all the spectral information into one single spectrum per object, resulting in a wavelength coverage of 3450 Å - 7450 Å. From these object, we choose NGC 2136 to apply our method. This is a SC located at the outskirts of the LMC (Figure 1).

✉ *Contact* / luisveganeme@gmail.com

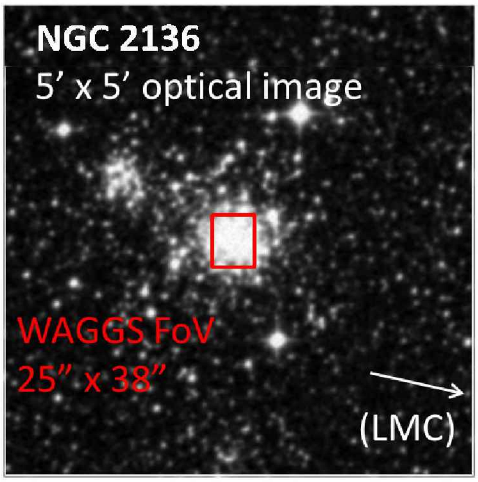

Fig. 1. Optical image of SC NGC 2136. North is up and East to the left. WAAGS FoV is marked by a red rectangle.

We use the spectral synthesis code `STARLIGHT` (Cid Fernandes et al., 2005) which combines theoretical Simple Stellar Populations (SSP) to model the observed spectra. This robust code was widely used for recovering the star formation history of galaxies, but only few times was applied to star clusters. The free parameters to fit are M_λ, *t*, A_V, and *[Fe/H]*. The formal combination of SSPs is performed as

$$M_\lambda = M_{\lambda_0}\left[\sum_{j=1}^{N_\star} x_j b_{j,\lambda} r_\lambda\right] \otimes G(v_\star, \sigma_\star) \quad (1)$$

where M_{λ_0} is the modeled flux at normalization wavelength λ_0, $N_\star$ is the number of components in the base of SSPs, x_j are the relative contributions of each SSP, $b_{j,\lambda} \equiv L_j(\lambda)/L_j(\lambda_0)$ is the spectrum of the j^{th} SSP normalized at λ_0, $r_\lambda = 10^{-0.4(A_\lambda - A_{\lambda_0})}$ is the reddening term, A_λ is the extinction law (Cardelli et al., 1989), and $G(v_\star, \sigma_\star)$ is a gaussian centered in velocity $v_\star$ with a velocity dispersion $\sigma_\star$. This latter term accounts for possible shift and broadening of the spectrum, but it is only important when dealing with massive systems (e.g. galaxies' bulges), which is not our case. The best model is found according to minimization:

$$\chi^2 \equiv \sum_{\lambda_i}^{\lambda_f} [O(\lambda) - M(\lambda)]^2 . \omega(\lambda)^2 \quad (2)$$

where $O(\lambda)$ is the observed spectrum, $\omega(\lambda)$ is a weight term (a zero value is used for masking; see below), and λ_i and λ_f are the initial and final wavelengths to fit, respectively.

The most usual base of SSPs comprises 150 spectra corresponding to 25 ages and 6 metallicities (Base "BC03"; after (Bruzual & Charlot, 2003)), which was built to take into account all possible values of age (from 10^5 to $2{\times}10^{10}$ yr) and metallicity (from -2.5 to 0.4). However, when dealing with SC, there is no need to include those SSP for which we know somehow they are not present. This is not an arbitrary decision: for instance, the inclusion of very young and/or metal-rich populations in globular clusters fittings would only oversample the SSPs and add erroneous estimates of the real properties of the object, besides being time-consuming runs. This sort of statistical noise could easily be avoided by using a sub-sample of BC03 base by choosing more "astrophysically important" SSPs, based on the previous estimates of the SC available in WAGGS sample (Usher et al., 2017). We thus made a customized base comprising ages from 10^6 to 10^9 yr and with solar, LMC and SMC metallicities.

To explore the dependence of the stellar population parameters with wavelength, we fit the spectra in certain ranges, increasing the coverage at steps of 100 Å from 3700 Å to 7000 Å, with a minimum initial range of 500 Å, thus performing $[29{\times}(29{+}1)/2] = 435$ fits per cluster according to the following scheme:

3700-4200				
3700-4300	3800-4300			
3700-4400	3800-4400	.		
3700-4500	3800-4500	..		
....	...	..	6400-6900	
3700-7000	3800-7000	..	6400-7000	6500-7000
(29 fits)	(28 fits)	..	(2 fits)	(1 fit)

The selection of the spectral regions to fit are done by masking the wavelengths outside of these regions. For instance, when fitting 3700 Å - 4400 Å we actually mask all data in 3450 Å - 3700 Å and 4400 Å - 7450 Å as WAGGS spectra goes from 3450 Å to 7450 Å. This is done by properly selecting $\omega(\lambda)$=0 in Eq. 2.

Finally, for each spectral range we obtain the mean values of age and metallicity by averaging over the SSPs parameters involved in the fits, by performing

$$< log(t) > \equiv \sum_{j=1}^{N} x_j \times (log(t_j)) \quad (3)$$

$$< [Fe/H] > \equiv \sum_{j=1}^{N} x_j \times ([Fe/H]_j). \quad (4)$$

3. Results

We applied the strategy described in the former section to NGC 2136. Figure 2 shows the fits with beginning wavelength in 4000Å covering just the blue part and the red part of the spectrum, respectively, along with some data derived from the synthesis. The extension of the fits outside the range (to the blue and red limits of the models) are shown to visualize the quality of the global fit, which in some cases are far from the observed spectrum, giving large global residues, despite the (local) good fit.

Figure 3 shows the behaviour of the age and [Fe/H] obtained for different ranges. The reference values

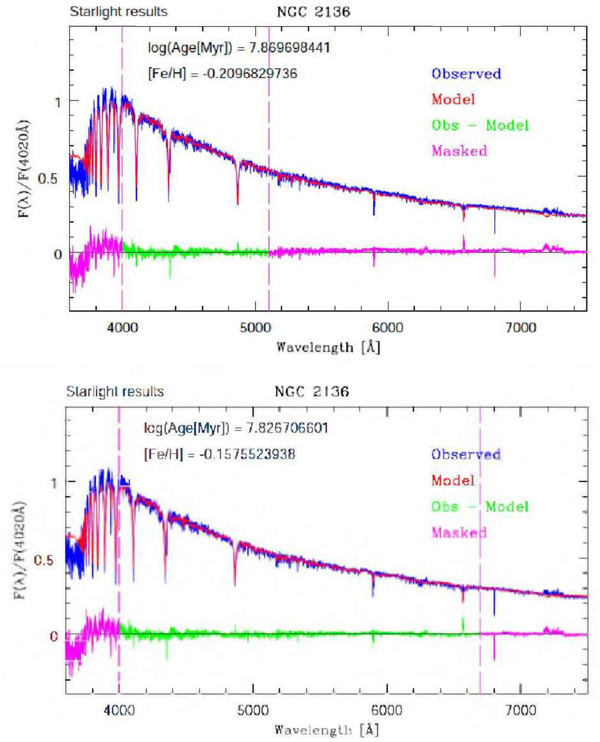

Fig. 2. Examples of fits with `Starlight` to the blue (*uppper panel*) and to blue+red (*bottom panel*) spectral regions.

(horizontal lines) for each parameter are taken from WAGGS. The colors denotes fittings with different starting wavelengths. Typical uncertainties are 0.1dex in log(age) and 0.2 in [Fe/H] (González Delgado & Cid Fernandes, 2010). In these plots, the examples mentioned in Figure 2 correspond to the blue line of Figure 3, i.e., λ_i=4000 Å. For these fittings, the resulting mean age and metallicity show no appreciable variation, regardless the covering region as long as the blue part is included. For the SC of our example, when considering λ_i=4000 Å the derived mean log(age)$\sim$7.8 and [Fe/H]$\sim$-0.15 are near and above the reference (literature) values, log(age)=7.8 and [Fe/H]=-0.37, respectively.

On the other hand, the results are different for the red spectral region (Figure 4): we obtained that the mean age and metallicity could be severely underestimated when the blue range is not included. This is evident for instance in the fittings with λ_i=5500 Å (red line) for which the mean log(age) and [Fe/H] decreases to $\sim$7 and $\sim$-0.6, respectively (see bottom right locii of Figure 3). Thus, we see that if only the red part is taken into account, some age and [Fe/H] sensitive absorption features are not considered, such as Hβ or Mg I lines: in this case the fit does not represent the global behavior despite the technical fact that the local residue is small.

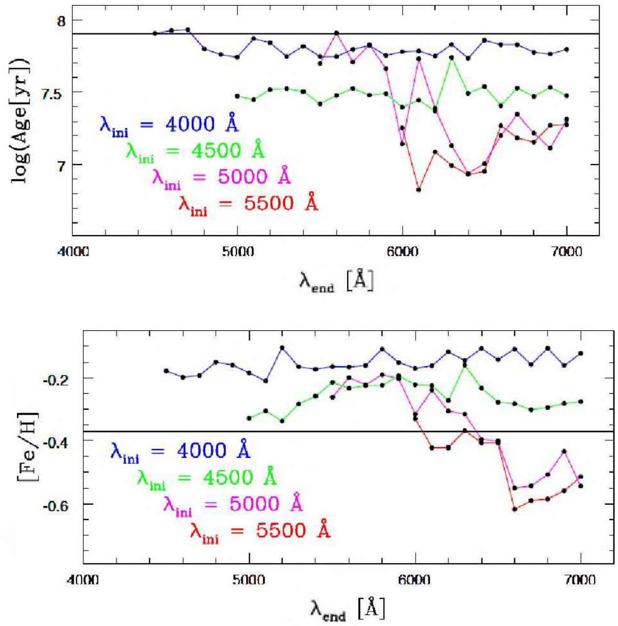

Fig. 3. Behaviour of mean log(age) (*upper panel*) and [Fe/H] (*bottom panel*) derived from `Starlight` fits applied to different spectral regions of NGC 2136. Each line connect values from different spectral range, beginning with λ_i and ending at λ_f, according to the scheme described in the text.

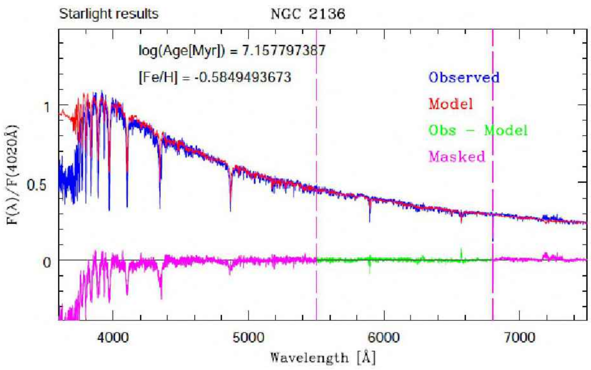

Fig. 4. Same as Figure 2 but for red spectral region.

References

Ahumada A.V., et al., 2019, PASP, 131, 024101

Bruzual G., Charlot S., 2003, MNRAS, 344, 1000

Cardelli J.A., Clayton G.C., Mathis J.S., 1989, ApJ, 345, 245

Cid Fernandes R., González Delgado R.M., 2010, MNRAS, 403, 780

Cid Fernandes R., et al., 2005, MNRAS, 358, 363

González Delgado R.M., Cid Fernandes R., 2010, MNRAS, 403, 797

Usher C., et al., 2017, MNRAS, 468, 3828

Vega Neme L.R., 2009, *Poblaciones estelares y mecanismo de ioniozación en núcleos activos de galaxias*, Ph.D. thesis, National University of Cordoba, Argentina

WAGGS; Usher C., et al., 2017, MNRAS, 468, 3828